



# UNIVERSITÀ DI PARMA

## ARCHIVIO DELLA RICERCA

University of Parma Research Repository

Hydrogel-thickened nanoemulsions based on essential oils for topical delivery of psoralen: Permeation and stability studies

This is the peer reviewed version of the following article:

*Original*

Hydrogel-thickened nanoemulsions based on essential oils for topical delivery of psoralen: Permeation and stability studies / Barradas, Thaís Nogueira; Senna, Juliana Perdiz; Cardoso, Stephani Araujo; Nicoli, Sara; Padula, Cristina; Santi, Patrizia; Rossi, Francesca; de Holanda e. Silva, K. Gyselle; Mansur, Claudia R. Elias. - In: EUROPEAN JOURNAL OF PHARMACEUTICS AND BIOPHARMACEUTICS. - ISSN 0939-6411. - 116:July(2017), pp. 38-50. [10.1016/j.ejpb.2016.11.018]

*Availability:*

This version is available at: 11381/2821567 since: 2021-10-25T15:29:46Z

*Publisher:*

Elsevier B.V.

*Published*

DOI:10.1016/j.ejpb.2016.11.018

*Terms of use:*

Anyone can freely access the full text of works made available as "Open Access". Works made available

*Publisher copyright*

note finali coverpage

(Article begins on next page)

## Title Page

# HYDROGEL-THICKENED NANOEMULSIONS BASED ON ESSENTIAL OILS FOR TOPICAL DELIVERY OF PSORALEN: PERMEATION AND STABILITY STUDIES

Thaís Nogueira Barradas <sup>1\*</sup>, Juliana Perdiz Senna <sup>1</sup>, Stephani Araujo Cardoso <sup>1</sup>, Sara Nicoli <sup>3</sup>, Cristina Padula <sup>3</sup>, Patrizia Santi <sup>3</sup>, Francesca Rossi <sup>4</sup>, K. Gyselle de Holanda e Silva <sup>2</sup> and Claudia R. Elias Mansur <sup>1</sup>

<sup>1</sup> Instituto de Macromoléculas Professora Eloisa Mano, Universidade Federal do Rio de Janeiro (IMA/UFRJ), Centro de Tecnologia, Bl. J, Avenida Horácio Macedo, 2030, Cidade Universitária, Ilha do Fundão – Rio de Janeiro – Brazil.

<sup>2</sup> Departamento de Fármacos e Medicamentos, Faculdade de Farmácia, Universidade Federal do Rio de Janeiro (UFRJ). Avenida Carlos Chagas Filho, 373, Cidade Universitária, Ilha do Fundão – Rio de Janeiro – Brazil.

<sup>3</sup> Dipartimento Farmaceutico, Università degli Studi di Parma, Parco Area delle Scienze 27/A, 43100 Parma, Italy

<sup>4</sup> Instituto IMEM-CNR, Parco Area delle Scienze 37/a, 43100 Parma, Italy

\* Correspondent Author

Thaís Nogueira Barradas

Instituto de Macromoléculas Professora Eloisa Mano, Universidade Federal do Rio de Janeiro (IMA/UFRJ), Centro de Tecnologia, Bl. J, Avenida Horácio Macedo, 2030, Cidade Universitária, Ilha do Fundão – Rio de Janeiro – Brazil, CEP: 21941-598.

[thaisbarradas@ima.ufrj.br](mailto:thaisbarradas@ima.ufrj.br). Tel: (+55) (21) 2562-7209

## ABSTRACT

Nanoemulsions (NE) have attracted much attention due to their as dermal delivery systems for lipophilic drugs such as psoralens. However, NE feature low viscosity which might be unsuitable for topical application. In this work, we produced hydrogel-thickened nanoemulsions (HTN) using chitosan as thickening polymer to overcome the low viscosity attributed to NE. The aim of this study is to develop and characterize oil-in-water (o/w) HTN based on sweet fennel and clove essential oil to transdermal delivery of 8-methoxsalen (8-MOP). NE components (oil, surfactant) were selected on the basis of solubility and droplet size and processed in a high-pressure homogenizer (HPH). Drug loaded NE and HTN were characterized for particle size, stability under storage and centrifugation, rheological behavior, transdermal permeation and skin accumulation. Transdermal permeation of 8-MOP from HTN was determined by using Franz diffusion cell. Transdermal permeation from HTN using clove essential oil showed strong dependency chitosan molecular weight. On the other hand, HTN using sweet fennel oil showed an unexpected pH-dependent behavior not fully understood at the moment. These results need further investigation, nevertheless HTN revealed to be interesting and complex dermal delivery systems for poorly soluble drugs.

Keywords: hydrogel-thickened nanoemulsions, permeation studies, essential oils, clove essential oil, sweet fennel essential oil, eugenol, *trans*-anethole, psoralens, terpenes, 8-MOP, Chitosan, transdermal delivery.

## 1- INTRODUCTION

Psoralens are naturally occurring tricyclic furocoumarins used, in association with ultraviolet light, in photochemotherapy (PUVA), a well-known treatment for psoriasis and vitiligo, which involves systemic or topical administration of psoralens and exposure of UVA light. PUVA can induce repigmentation by stimulation of melanogenesis, immunomodulation and activation of growth factors, though the exact mechanism is still unknown [1]. Among psoralens (8-methoxypsoralen (8-MOP), 5-methoxypsoralen (5-MOP) and 4,5',8-trimethylpsoralen (TMP)) 8-methoxsalen (8-MOP) is the most widely used in PUVA therapy [2].

Psoralens are lipophilic molecules with logP between 2 and 3, and are therefore, in principle, suitable for oral and topical administration. However, systemic treatment presents many drawbacks, such as liver carcinogenicity, tachycardia, herpes simplex, depression and insomnia, among others. The topical treatment, despite being a safer approach, has limitations related to intense local phototoxicity and slow therapeutic effect, due to insufficient drug penetration into the skin layers [3–5].

When activated by ultraviolet radiation (200 to 400nm), psoralens cause phototoxic reactions in the epidermis with an intensity which can vary according to the concentration and exposure time [6–8]. The oral therapy with psoralens is related to the high frequency of toxicity, such as liver carcinogenicity. The most frequent side effect is acute phototoxicity, similar to severe sunburn and may persist for days, followed by systemic effects such as tachycardia, herpes simplex, fever, nausea, headache, dizziness, depression and insomnia, unusual rashes with pain and deep distress in the skin. Psoralens can also reach the eyes and interact with proteins of retina, causing opacity, conjunctival changes and early cataracts, which makes this treatment unsuitable for children under 12 years. For this reason, the eye photoprotection must be emphasized during the treatment [5,10,11].

In the long term, phototherapy can cause photoaging, hepatotoxicity and liver damage, renal toxicity, hypertension, hyperlipidemia and immunosuppression. The risk of carcinoma and melanoma is by an average of 2.6 times higher than the rest of the population. Furthermore, the psoralens have the ability to inhibit enzymes of the P450 2A6 cytochrome family, responsible for the metabolism of numerous substances and drug [10–13].

In the intention to reduce the systemic effects of oral therapy, topical PUVA has become an alternative. Topical PUVA does not produce systemic effects, enhances the therapeutic effects of the treatment of various dermatoses and does not require prolonged ocular photoprotection [14,15].

However, the local phototoxicity is intense and fast, being a dose-dependent phenomenon. Adverse effects are usually immediate such as erythema, edema and vesicles that occur due to uncontrolled psoralen photoreaction in the epidermis with radiation because the drug is freely available in the dosage form to react with the skin surface after topical application [16,17].

Besides the cases of toxicity, topical treatment with psoralen imposes complications since these drugs have low penetration capacity into the deeper skin layers, which requires the administration of higher doses and increased exposure time to UVA radiation, increasing the risk of serious adverse effects such as carcinogenesis [5,18,19].

It is well known that the vehicle in which a certain drug is included has a significant effect on its dermal or transdermal penetration. In general, it is possible through a careful selection of vehicle components to optimize skin penetration of an active molecule. Over recent years, several nanosystems have been proposed in order to increase the penetration of psoralens across the skin [20–23]. Among them, nanoemulsions are the most commonly used, for their ability to favor dermal drug penetration. In addition, several authors have demonstrated that it is possible to control drug release and skin permeation by adjusting the formulations, enabling dose reduction and, therefore, reducing adverse effects [5,24,25]. Another strategy to increase drug permeation through the skin is the addition of permeation enhancers, including terpenes, especially those of vegetable origin, which are described as a class of products with low toxicity, low irritation potential and listed in insurance excipients FDA [26,27].

One of the disadvantages of the use of nanoemulsions for topical application is the low viscosity, which limits their clinical application and makes their topical administration inconvenient. In this context, the development of a hydrogel-thickened nanoemulsion, by the introduction of a gel-forming polymer to the outer phase of the formulation, can solve this disadvantage and make the nanoemulsion suitable for topical application [28–31]. Such system can combine the characteristics of stability and skin penetration of nanoemulsions with the properties of sustained drug release of hydrogels thus optimizing the therapeutic effects and allowing a reduction of the dose [32,33].

One of the polymers more suitable for topical application is chitosan, a semisynthetic polymer capable of forming hydrogels by entanglement of polymer chains which entrap a large amount of water molecules, swelling in the presence of this solvent. In particular, chitosan hydrogels show mucus and bioadhesion properties, capable of increasing drug residence time on the skin and promote drug skin penetration. This is due to the cationic nature of chitosan, which allows its polymeric chains to establish ionic interactions with the surface of the

*stratum corneum*. Such characteristics make hydrogels based on chitosan good candidates for the development of dermal drug delivery systems [34–36].

This paper proposes the development of chitosan-thickened nanoemulsions containing essential oils rich in terpenes, for the topical application of 8-MOP. The effect of different surfactants (Pluronic and Cremophor) as well as of the presence and viscosity of chitosan was evaluated as well.

## 2- EXPERIMENTAL PART

### 2.1 *Materials*

The materials used in this study were: the psoralen 8-methoxysalen (1, MW= 216.2 g/mol, m.p. = 142–148 °C, Xanthotoxin, 99% purity) was used as received Sigma-Aldrich, São Paulo, Brazil; Sweet Fennel, Peppermint, Orange, Lime, Buriti, Avocado, Clove and Copaiba essential oils obtained from Ferquima, São Paulo, Brazil; cellulose acetate membrane (pore size of 0.2 µm), acquired from Sigma-Aldrich, Missouri, USA; the poly(ethylene oxide)-poly(propylene oxide) block copolymer, Pluronic F68, obtained from Sigma-Aldrich, Missouri, USA; Cremophor RH 40 (PEG-40 hydrogenated castor oil), obtained from Oxiteno, São Paulo, Brazil and Chitosan of low (50,000 - 190,000 Da), medium (190,000-310,000 Da) and high (310,000 to 375,000 Da) molecular weight obtained from Sigma-Aldrich, Missouri, USA. All Chitosan grades were at least 75% deacetylated according to the supplier.

### 2.2 *Methods*

#### 2.2.1 *Screening of oil phase*

Due to its low water solubility, 8-MOP was subjected to preliminary solubility tests in various oil concentrations of 1 - 20% w/v. Therefore, we employed canola, almond, grape seed, avocado and buriti, copaíba, lemongrass, lime, sweet fennel, lemon balm, mint, clove (stem and button) and orange vegetable essential oils. For this purpose, we performed a preliminary selection of essential oils by visual observation of solubilization of 8-MOP using a qualitative criterion based on the United States Pharmacopeia (USP) in the chapter entitled “Description and Relative solubility” [37].

1 mg of 8-MOP was added to 1 mL of each essential oil mentioned above. Then, the systems were subjected to ultrasonic cavitation to accelerate solubilization for 15 minutes, and solubility was assessed visually after 24 hours. To the oils that promoted solubilization, the above procedure was repeated consecutively until the observation of precipitation for each system.

The essential oils in which 8-MOP had higher solubility classification were chosen to be evaluated quantitatively by Ultraviolet (UV) spectrophotometry. The determination of 8-MOP concentration was performed in sweet fennel and clove essential oils. The samples for determining the solubility were prepared by adding an excess quantity of 8-MOP to a defined volume of each essential oil. These suspensions were kept under stirring for 24 hours at room temperature ( $25 \pm 1$  °C), after which the suspensions were centrifuged at 3,000 rpm for 5 minutes. Then the supernatant was removed with the aid of a Pasteur pipette and each sample was filtered through cellulose filter element. An aliquot of each solution was diluted with ethanol and subsequent dilutions were prepared in ethanol. The absorbance of these solutions was determined using quartz cuvette (1 cm) and wavelength 300 nm, a calibration curve was prepared in ethanol.

### 2.2.2 *Development of NE containing 8-MOP*

The formulations were produced by employing a high energy was performed by means of a high-pressure homogenizer (HPH). The concentration of 8-MOP in the formulation was 0.05% w/w in accordance with the systems produced by Lai *et al.*, (2008) submitted to sonication for 15 minutes to ensure complete solubilization of the drug. The proportion of oil phase was 5% w/w. All formulations were processed in high pressure homogenizer (HPH), EmulsiFlex C5, chosen as a high energy method to obtain NE. Samples were processed for 5 cycles and 1500 bar at 25 °C.

### 2.2.3 *Preparation of hydrogel- thickened nanoemulsions (HTN) based on chitosan*

In this study, 2% w/w of chitosan with high, medium and low molecular weights were added to the outer phase of the NE, which had their pH adjusted with acetic acid solution 1% v/v. Sufficient amount of chitosan was slowly added to the systems under magnetic stirring until complete dispersion providing HTN based on chitosan. The NE, template for the production of these systems, have been selected according to the average droplet diameter and the physicochemical stability of the systems. The compositions of all samples produced in this study are shown in Table 3.

### 2.2.4 *Hydrodynamic size and stability under storage*

The hydrodynamic size and polydispersion index of the processed formulations were determined by dynamic light scattering, in a Zetasizer Nano ZS (Malvern Instruments, UK). These measurements were performed on samples of approximately 10  $\mu$ L of the dispersions,

which were diluted in 1 mL of recently distilled and deionized water. The measures were conducted at room temperature (25 °C), using a laser incidence angle in relation to the sample of 173° and a 5 mL quartz cuvette. The values reported correspond to the mean  $\pm$  standard deviation (SD) of three measurements of each formulation. The polydispersity index, calculated by the device, reflects the homogeneity profile of the diameter of the sample's droplets. A polydispersion index under 0.3 was considered satisfactory. The measurements were conducted for all the samples immediately after processing and again at intervals of 1, 2, 3, 4, 8 and 12 weeks to study the formulations' stability.

### 2.2.5 *Physical Stability Studies*

All formulations were subjected to different stability tests to assess their physical stability. The evaluation of organoleptic aspects was carried out subjectively by comparing all samples subjected to different storage conditions. It was defined as reference the sample kept at room temperature. For the evaluation of appearance, alteration levels observed were classified into (I) normal, without alteration; (II) slightly precipitated or slightly turbid and (III) phase separation, precipitate or cloudy. The degree of color and odor alterations observed in the formulation was classified according to the following criteria: (I) Normal without change; (II) slightly modified; (III) modified and (IV) intensely modified.

#### 2.2.5.1 *Stability under freeze/heating cycles:*

NE and HTN were subjected to alternate freeze and thaw cycles, 24 h each, for a period of 12 days. The samples were stored at 4.0°C for 12 h then at 45.0°C for the same period of time. At the end, the samples were left over night to recover and equilibrate at room temperature. Signs of physical stability, for example, transparent appearance, pH and droplet size, were re-assessed.

#### 2.2.5.2. *Centrifugation test*

Formulations were heated for 24 hours and then, centrifuged first at 11.000 rpm for 30 min each time, and we evaluated phase separation by visual inspection.

#### 2.2.5.3 *Stability under thermal stress*

Samples (triplicate) were placed in flasks with hermetically sealed cover. The total volume of the flask was not completed to allow gas exchange possible. The samples were

submitted to heating in stove at  $45 \pm 2$  ° C for 90 days. Control samples were kept at room temperature for the same period of time. The evaluation of the samples was performed initially at time zero and after 15, 30, 60 and 90 days. We evaluated organoleptic (color, odor and appearance) and physicochemical (pH, droplet size and viscosity) parameters.

#### 2.2.5.4 *pH determination.*

The pH values of formulations were determined in triplicate directly in the samples (Oakton Ion6 potentiometer).

#### 2.2.5.5 *Shear viscosity measurements*

Measurements were performed in a dynamic shear rheometer (HaakeRheoStress 600, Thermo Electron Corporation) equipped with a cone-plate geometry with a cone diameter of 35 cm and angle of 1° and a gap of 0.052 mm. Temperature (25°C) was controlled by a Phoenix II cooling and heating system ( $\pm 0.1$ °C). The reliability of measurements was assured by obtaining the rheograms in triplicate. Flow curves were determined with two consecutive continuous shear rate ramps from 1 to  $150 \text{ s}^{-1}$  with ascending and descending cycles.

#### 2.2.5.6 *Quantification of 8-MOP by high performance liquid chromatography (HPLC)*

8-MOP content in samples was determined using an HPLC system (Perkin-Elmer, Norwalk, CT) and a NovaPak® C18 column ( $150 \times 3.9$  mm, Waters, USA). Samples were eluted with a mobile phase consisting of methanol:water (65:35 v/v), The flow rate was 0.7 mL/min UV absorption was monitored at 300 nm and the run time was about 5 minutes using the method previously developed by Colombo et al., (2003) [38].

A stock solution was prepared by dissolving weighed amount of 8-MOP in methanol. Five solutions were obtained with appropriate dilution of the stock solution with methanol, to give concentrations in the 15.0, 25.0, 35.0, 45.0 and  $50.0 \mu\text{g mL}^{-1}$ . The analyses were conducted in triplicate.

### 2.2.8 *Transdermal drug permeation studies*

#### 2.2.8.1 *Skin samples preparation.*

Pig ears were obtained from a local slaughterhouse immediately after the death of the animal. Full thickness skin was excised from the outer region of the ear and separated from the underlying cartilage with a surgical blade. Hairs were trimmed carefully with scissors.

After the removal of subcutaneous fat, the skin was wrapped in aluminum foil and stored at  $-20^{\circ}\text{C}$  until use and used within 3 months.

#### 2.2.8.2 Permeation experiments

Permeation experiments were conducted in vertical Franz-type diffusion cells (Disa, Milan, I), with an exposed surface area of  $0.6\text{ cm}^2$  using full-thickness pig ear skin as barrier. The donor compartment was filled with  $500\text{ }\mu\text{L}$  of NEs prepared. As reference a  $0.05\%$  w/w 8-MOP solution in ethanol was used. Although ethanol is well known as skin permeation enhancer, it was used because it has been often the main vehicle for 8-MOP.

The receptor phase was filled with  $4\text{ mL}$  of  $0.9\%$  sodium chloride solution and  $1\%$  wt of  $\beta$ -cyclodextrin, thermostatted at  $37^{\circ}\text{C}$  and magnetically stirred in order to prevent any boundary layer effects. At predetermined time intervals the receptor solution was sampled and analyzed by HPLC for the determination of drug permeated. Each permeation experiment lasted  $6\text{ h}$  and was replicated at least 6 times using skin from different animals. At the end of this period of time, the excess amount of the formulation was removed and the skin surface was cleaned with dry paper and isopropyl alcohol. SC and epidermis were separated from dermis with heat application [39]. All samples were weighed and inserted in vials. 8-MOP was extracted from the skin layers using  $1\text{ mL}$  of a methanol:water ( $60:40$ , v/v) mixture. The amount of 8-MOP was determined by HPLC.

The extraction method was validated in blank experiments and by spiking with a known amount of 8-MOP. In all cases, no interfering peaks derived from skin samples were detected. The recoveries were above  $90\%$  from both epidermis and dermis. 8-MOP skin concentration was calculated by normalizing the amount of drug recovered in the *stratum corneum* + epidermis and dermis by the weight of tissues and expressed as  $\mu\text{g}$  of drug per mg of tissue. Each experiment was replicated 6 times.

Permeation profiles obtained were then fitted to Fick's Second Diffusion Law mathematical model (Equation 1) [40], where  $Q$  is the cumulative amount of drug permeated per unit area at time  $t$ ,  $C_{\text{veh}}$  the concentration of the drug in the donor vehicle,  $K$  the stratum corneum/vehicle partition coefficient,  $D$  the diffusion coefficient and  $H$  the diffusion path-length. The permeability coefficient  $P$  was calculated as the product between  $KH$  and  $D/H^2$ . The fitting was performed using KaleidaGraph<sup>®</sup> 3.6.2 (Synergy Software).

$$Q = (KH)C_{\text{veh}} \left[ \frac{D}{H^2}t - \frac{1}{6} - \frac{2}{\pi^2} \sum_{n=1}^{\infty} \frac{(-1)^n}{n^2} \exp\left(\frac{-Dn^2\pi^2t}{H^2}\right) \right]$$

### 2.2.8.3 Skin retention experiments

To evaluate the amount of 8-MOP accumulated in skin layers (Stratum Corneum + epidermis and dermis) skin retention experiments were conducted in Franz's type diffusion cells in similar conditions of permeation experiments. NEs were applied in finite dose conditions (10  $\mu\text{L}/\text{cm}^2$ ) and left in contact with the skin for 2 h. At the end of this period of time, skin samples were treated and extracted as described above.

### 2.2.8.4 Transmission Electron Microscopy (TEM)

The surface morphology of NEs were observed using an JEOL 2200-FS electron microscope operated at 80 kV. NEs samples were deposited on a copper mesh grid. After 60 sec the excess of fluid was removed with filter paper. Staining was obtained with 2% phosphotungstic acid aqueous solution. Samples were left to dry overnight and then observed.

### 2.2.8 – Data analysis

All the statistical tests were repeated three times and expressed as the mean  $\pm$  SE using Origin Pro 8 (OriginLab, USA) software.

## 3 – RESULTS AND DISCUSSION

### 3.1 Screening of oil phase

8-MOP (Log P = 1.93) [41] is a soluble drug in ethanol, and freely soluble in chloroform, sparingly soluble in water ( $< 4 \times 10^{-4}\text{M}$  concentration can be achieved). The maximum solubilization capacity of 8-MOP in each essential oil was studied and the results are shown in Table 1. For this, the oil phase of the NE produced was preselected by visual observation of solubilization of 8-MOP in different essential oils. According to apparent solubility, it was possible to choose the best components essential oils for constituting the oil phase: Clove (*Eugenia caryophyllus*) and sweet fennel (*Foeniculum vulgare Mill.*) essential oils (Table 1). Once these were oils with higher drug solubilization capacity in the study, we performed the quantitative evaluation regarding the ability of each one to solubilize 8-MOP. Clove oil proved to be more effective in promoting 8-MOP solubilization ( $4.42 \pm 0.23 \text{ mg/mL}$ ) compared to sweet fennel essential oil ( $1.46 \pm 0.13 \text{ mg/mL}$ ).

### 3.2 Production of NE

The right selection of surfactants is essential, since the most critical problem related to nanoemulsion-based systems is the toxicity of their components which might cause skin irritation. In this paper we employed non-ionic surfactants and hydrophilic, and which are widely used for pharmaceutical purposes due to their low toxicity and greater stability against changes in ionic strength and pH in biological environments [42]. Furthermore, the HLB of the selected surfactant ( $> 10$ ) provided the formation of nanoemulsions with hydrophilic outer phase. The composition of each formulation is shown in Table 2. The selection of the surfactant was based on the composition that produced samples with smaller droplet size after HPH processing and stabilization promoted by the lower amount of surfactant possible (data not shown). From preliminary studies, we selected Pluronic F68 at a concentration of 10% w/w for the formulations containing clove oil as oil phase, based on previous results obtained by our research group [43], and for formulations containing sweet fennel essential oil was used Cremophor RH40 at 3% w/w.

### *3.3 Dynamic light scattering experiments*

According to Gupta et al., (2016) [44] droplet size distribution of an emulsion impacts many properties such as long-term stability, texture and optical appearance. Measurements of droplet size by dynamic light scattering were performed for NE containing both clove and fennel essential oils, after HPH processing and before adding chitosan.

NE containing clove oil and Pluronic F68 as single surfactant were produced with the aid of a HPH for 5 processing cycles at 1500 bar pressure and showed kinetic stability for at least 3 months (Figure 1). The surfactant plays an essential role in decreasing droplets size and also in maintaining droplets size and steric stabilization of formulations [45]. Block copolymers as PEO-PPO-PEO, as used in this work, tend to self-organize into micelles brush shaped, being able to perform effective steric repulsion [46] .

Other authors published their results when developing NE and microemulsions with clove oil. However, they used mixtures of surfactants, co-surfactants and often small molecules such as Tween and Span as surfactants. Moreover, they obtained formulations with larger average droplet diameter compared to those obtained in this work. Besides, they reported changes in droplet size over time and also, a high surfactant/ oil proportion [47–50].

Previously, NE containing sweet fennel oil were produced for the most varied applications [51,52]. However, their work also used high concentrations of surfactants which may

cause skin irritation problems. In this paper, we present an alternative to the production of NEF by HPH with the use of a single non-ionic surfactant (Cremophor RH40) at a concentration of 3% w/w. Such a low surfactant concentration for achieving stable NE is not common in the literature. However, this can be explained by the self-emulsification intriguing called "ouzo effect" [53]. This phenomenon can act synergistically to the stable NE production process and favor the use of lower concentrations of surfactant, which explains the large difference surfactant concentration necessary for the production of NE containing clove and sweet fennel essential oils. Carteau *et al.*, (2008) [53] reported the obtention of spontaneously formed microemulsions produced by diluting solutions ethanolic content trans-anethole without using surfactants.

Samples were evaluated during 12 weeks in order to analyze size and PDI of dispersed droplets. After processing, all formulations displayed a relatively narrow size distribution range with PDI values less than 0.2, suggesting the high-energy method employed for the production of NE was well succeeded, which resulted in droplets of  $68.1 \pm 0.6$  nm for sweet fennel-based NE and  $91.3 \pm 0.3$  nm for clove-based NE during at least 3 months (12 weeks) (Figures 1 and 2).

### 3.4 Stability under freeze/heating cycles

NE based on clove oil and sweet fennel essential oil (NEC and NEF, respectively) formulated in the absence of chitosan and their HTN formulated with low, medium and high molecular weights of chitosan, were submitted to preliminary stability studies. The samples were examined macroscopically and subjected to pH, organoleptic parameters and droplet size. The results are shown in Table 3 and Figures 3 and 4.

The organoleptic tests allowed assessing the samples by comparative analysis, in order to verify changes regarding to color, odor and appearance. It was found similarity of the formulations subjected to stability tests in relation to the newly developed, regardless of the conditions and storage periods. We performed centrifuge tests at 11,000 rpm to assess samples behavior under increased centrifugal force. All formulations subjected to preliminary stability tests showed similarity with regard to color, odor, and appearance, compared to control formulation, regardless of storage conditions. Furthermore, the formulations submitted to centrifuge tests showed no visible turbidity and cremation or phase separation. All tested formulations appeared to maintain their initial characteristics under alternating storage conditions

according to macroscopic visual evaluation. Furthermore, the average droplet size of NEF and NEC subjected to centrifugation (Figure 4) was similar to that observed for NE freshly prepared with a gaussian distribution for both formulations, suggesting uniformity of droplet size under such conditions. However, the same was not observed for the NEC after the heating and freezing cycles. A new population of droplets with average size of about 3000 nm was formed after heating and freezing cycles, which can be explained by the thermosensitive behavior attributed to PEO-PPO block copolymers, due to the limited water solubility of PEO segment, which is extremely sensitive to increasing temperature [54,55].

It is likely that this phenomenon has led to decreased solubility of the surfactant used to stabilize the NEC, which would induce the approximation of droplets with consequent spontaneous coalescence between them in order to decrease the extent of the oil/water interface. This destabilization initial sign was not detected macroscopically. HTN formulations were not evaluated as to the droplet size, since the presence of large polymeric chains of the chitosan prevented the proper dynamic light scattering measurement and probably would interfere in oil droplets size measures. Given the relative stability demonstrated in preliminary studies, the systems were subjected to accelerated stability studies over a period of 90 days.

### 3.5 *Stability under thermal stress*

Given the relative stability demonstrated in preliminary studies, the systems were subjected to accelerated stability studies over a period of 90 days. It was observed up to 30 days at high temperature of 45 °C, the formulations showed no destabilization signs, color or odor alterations (Table 4). However, after 60 days exposed to high temperature, there was slight change in coloring of HTN formulations obtained from the clove essential oil, which became darker. At the end of 90 days all HTN containing clove oil showed strong brownish, suggesting oil oxidation. The same was not true for the NEC in the same time period, suggesting that under these conditions the interaction between chitosan and, NE constituents can speed up the process of destabilizing HTN containing essential oil of clove.

#### 3.5.1 *pH determination*

The pH of a formulation should guarantee the stability of the formulation ingredients, also their effectiveness and safety as well as be compatible with biological tissues according to the intended route of administration [56]. The average pH values for formulations contain-

ing oil of fennel showed no significant difference ( $P > 0.01$ ) when analyzed by ANOVA, suggesting that formulations feature reasonable physicochemical stability when subjected to 90 days of continuous exposure to heat (Figure 5). However, the evaluation during 90 days showed a significant decrease in pH of all formulations containing clove oil from the 30th day on. The change in pH value was greater for the formulations presented higher initial acidity, suggesting that reducing the pH of HTN to facilitate solubilization of chitosan can accelerate destabilization. This observation may reflect the oil phase oxidation phenomenon with hydroperoxide formation or the hydrolysis of triglycerides with the formation of fatty acids, responsible for the pH decrease of the formulations.

### 3.5.2 *Shear viscosity measurements*

The evaluation of viscosity helps to conclude whether a product provides proper consistency and viscosity and can indicate if stability is adequate, i.e. can indicate product behavior over time [57]. Moreover, instabilities arising from variation in size, particle number and emulsifier orientation or migration over a period of time can be detected by changes in the apparent viscosity of the product .

All HTN exhibited pseudoplastic flow (Figures 6 and 7), i.e. the viscosity decreasing with increasing applied shear stress. This behavior is desired in pharmaceutical formulations for preventing the mobility of the dispersed phase under low shear stress, being important that it exhibits free flow when shaken, showing low viscosity compared to high shear rates, these being reversible changes after certain time repose, delaying coalescence or creaming [44]. The reduction in viscosity when increasing shear rate is associated with the entanglements or physical nodes, responsible for raising the viscosity of formulation, for obstructing the flow system. With increasing shear rate, such physical nodes are broken and polymer chains align in the direction of the applied strain, which is responsible for reducing the viscosity under these conditions [58].

Indeed, the addition of chitosan altered the rheological behavior of HTN compared to control (non-gelified NE) in all cases. NE showed low viscosity and newtonian behavior regardless the shear rate applied. In general, it was noticed an increase in viscosity of HTN, as the chitosan molecular weight increases. During this 90 days test, HTN showed marked decrease in apparent viscosity. These data are consistent with previous studies indicating decrease of viscosity of aqueous solutions and gels of chitosan as temperature increased [59,60].

Mironov et al., (2007) [61] reported a decrease in dynamic viscosity of solutions of chitosan in acetic acid during the storage, which would be related to polymer degradation phenomena with consequent reduction of its molar mass, which is reflected in the viscosity of chitosan based systems. Thus, temperature associated with the low pH of HTN, possibly caused degradation reactions of chitosan, which may explain the decrease in viscosity over time of study.

In general, all the results observed in this study may be related. Oxidation oil phase could lead to the formation of acidic species which could be responsible for the accelerated degradation of chitosan polymer chains. This phenomenon was reflected in both the color alterations of HTN and also when assessing the viscosity of chitosan-based HTN. Thus, the accelerated stability study showed that the NE were able to maintain their initial appearance even facing extreme conditions of storage. No typical instability sign such as flocculation, creaming or phase separation were visible. The droplet size distribution of NE stored at 45°C is shown in Figure 8. The analysis of droplet size profile of NEF demonstrates a unimodal distribution of formulations submitted to heating. Samples composed on clove essential oil showed a bimodal distribution in droplet size distribution after 30 days of storage with a large peak at about 90 nm and a small peak at about 4000 nm, suggesting coalescence and characterizing instability of these NE submitted to these storage conditions.

### *3.6 Permeation Studies*

The permeation of 8-MOP was studied in vitro using porcine skin, a well-known and accepted model of human skin. The formulations studied were constituted by a “control sample” (0.05 % w/v solution in ethanol), the prepared NE and their correspondent hydrogel-thickened systems, containing either clove oil or fennel oil as dispersed phase and as penetration enhancer. Since oil phase constituents were different, formulations differed also regarding the surfactant used, i.e. Pluronic F68 vs. Cremophor RH40. The effect of the presence of chitosan of different molecular weights was studied as well.

In the case of clove oil (Figure 9), the control sample provided a higher permeation profile compared to the plain NE: The addition of chitosan further reduced 8-MOP permeation, probably because to the higher viscosity of the formulation. It is interesting to observe that the difference between the control formulation and the plain NE was only in the early time of the experiment, suggesting a similar permeability but a longer time-lag to reach steady-state for the NE.

This behavior was reversed in the fennel oil containing NEF: the control sample was almost superimposed with the plain NE but the addition of chitosan increased 8-MOP penetration, to reach the maximum level when high molecular weight chitosan was used.

Both NEF and NEC contained different penetration enhancers, i.e. clove oil containing eugenol and sweet fennel oil containing *trans*-anethole. It is well known that enhancing properties of a given penetration enhancers depends on the permeant, however, there are reports in the literature that indicate a higher efficiency of *trans*-anethole compared to eugenol [62]. This is in agreement with the higher permeation of NEF compared to NEC.

Another difference between the two NE is the surfactant: Cremophor RH40, contained in the sweet fennel oil NE, is a non-ionic surfactant known in the literature for its ability to alter *stratum corneum* lipid arrangement: the presence of this enhancer can explain the slight, although not significant, increased permeation from such a formulation.

Incidentally, it should be considered that clove oil-based NE show slightly larger droplet size compared to fennel oil-based formulations ( $68.1 \pm 0.6$  nm vs.  $91.3 \pm 0.3$ ), although the relevance of this difference is not easy to predict.

Table 4 reports all permeation parameters calculated for all formulations. The permeation profiles of 8-MOP were generally not linear with time, suggesting that steady-state conditions were not achieved over the duration of the experiment. For this reason, the approximate solution of Fick's second law [40] was applied, to calculate the relevant permeation parameters, such as partitioning parameter (KH), diffusive parameter ( $D/H^2$ ) and permeability coefficient (P): KH gives indications of the partitioning of the permeant between the *stratum corneum* and the formulation, whereas the diffusive parameter gives indication of the overall diffusivity of the molecule. The lag time (*T lag*) values were determined from the x-intercept of the slope at a steady state.

On first inspection it is evident that the formulations containing sweet fennel oil and Cremophor RH40 (NEF-NHF) showed higher permeability coefficients, whereas those containing clove oil and Pluronic F68 the opposite: the addition of chitosan reduced the permeability coefficient in NEC whereas increased it in NEF. The analysis of the diffusion and partitioning parameters revealed that the partitioning parameter was the one modified, whereas the diffusive parameter remained more or less constant. The partitioning parameter increased slightly in the plain NEF, containing sweet fennel oil and Cremophor RH40, but the increase

was more evident in the NHF formulation, containing chitosan ( $p < 0.01$  compared to the control).

Figure 12 presents 8-MOP skin accumulation from formulations based on clove (A) and sweet fennel essential oil (B) under finite dosing. As expected, the epidermis accumulation was higher than dermis accumulation in all cases. NEC formulation accumulated more 8-MOP in both tissues compared to the control formulation: this skin retention decreased in the presence of chitosan, following the same trend as the permeation profile. The higher retention from the plain NEC compared to control is in line with the higher partitioning parameter found; the same trend was found also for the presence of chitosan. Using NEF and NHF formulations the situation was completely reversed, because the retention increased with the presence of chitosan, as penetration did.

In order to try to understand the results obtained, in particular the effect of chitosan TEM images of the prepared systems NEC and NEF were taken (after negative staining with phosphotungstic acid). The results are reported in Figure 13.

The image reported in Panel A, relative to the formulation containing clove oil and Pluronic as surfactant, is typical of NE, with the presence of small lipid droplets, surrounded by a layer of surfactant (Pluronic F68) which stabilizes the structure. The particle size that can be estimated from the image is bigger than the value obtained by DLS upon dilution; this can be an artifact of sample preparation for TEM analysis (dehydration, droplet flattening).

On the contrary, the structure reported in Panel B, sweet fennel oil dispersed in water using Cremophor RH40 as surfactant, does not look like a NE but perhaps more as a bicontinuous NE, wherein small domains of oil and water are inter dispersed. Upon addition of water, bicontinuous phases generate NE, as demonstrated by the particle size measurement of the diluted sample. It has been reported that bicontinuous microemulsions are dynamic structures with continuous fluctuations occurring between the bicontinuous structure, swollen reverse micelle and swollen micelles and for this reason they may improve drug penetration across the skin [63]. The TEM images of chitosan containing formulation NHF show a significant change in the structure: the systems appears more like a very fine NE (note that in the presence of chitosan, phosphotungstic acid binds to the polymer), which is probably more efficient in delivering 8-MOP to the skin.

Finally, the skin retention experiments on NE were replied in conditions similar to those used in therapy, i.e. in finite dose conditions for 2 hours of contact time: no control

formulation as used, because in finite dose conditions ethanol evaporates quickly leaving the solid drug on the skin surface (Figure 13). The results obtained in finite dose conditions are similar to those obtained in infinite dose conditions, although generally lower. 8-MOP was found in the receptor compartment only the case of NHF2 and NHF3.

#### 4- CONCLUSIONS

The incorporation of 8-MOP into two NE containing essential oils (either sweet fennel or clove essential oil) as oil phase lead to the development of formulations with which it was possible to modulate transdermal drug delivery and skin retention. In particular, the use of clove oil, associated with Pluronic F68, led to a reduced skin permeation and increased skin retention, also in the presence of chitosan as thickener. This formulation is very promising for the PUVA therapy, because it guarantees high efficacy and low systemic exposure to the drug. On the contrary, the formulation containing sweet fennel oil, associated with Cremophor RH40 and thickened with chitosan, allowed higher skin penetration and retention. The effect produced by addition of chitosan was completely unexpected and it is worth further studies to elucidate the exact mechanism of interaction.

#### 5- ACKNOWLEDGMENTS

We thank the Office to Improve University Personnel (CAPES), of the Ministry of Education and the National Council for Scientific and Technological Development (CNPq) .

## References

- [1] A.D. Buhimschi, F.P. Gasparro, UVA and UVB-Induced 8-Methoxypsoralen Photoadducts and a Novel Method for their Detection by Surface-Enhanced Laser Desorption Ionization Time-of-Flight Mass Spectrometry (SELDI-TOF MS), *Photochem. Photobiol.* 90 (2014) 241–246.
- [2] F.A. de Wolff, T. V Thomas, Clinical pharmacokinetics of methoxsalen and other psoralens., *Clin. Pharmacokinet.* 11 (1986) 62–75.
- [3] V.N. Sehgal, G. Srivastava, Vitiligo treatment options: An evolving scenario, *J. Dermatolog. Treat.* 17 (2006) 262–275.
- [4] L.M. Felsten, A. Alikhan, V. Petronic-Rosic, Vitiligo: A comprehensive overview, *J. Am. Acad. Dermatol.* 65 (2011) 493–514.
- [5] K. Borowska, S. Wołowiec, K. Główniak, E. Sieniawska, S. Radej, Transdermal delivery of 8-methoxypsoralene mediated by polyamidoamine dendrimer G2.5 and G3.5--in vitro and in vivo study., *Int. J. Pharm.* 436 (2012) 764–70.
- [6] Z. Zarebska, E. Waszkowska, S. Caffieri, F. Dall'Acqua, PUVA (psoralen + UVA) photochemotherapy: processes triggered in the cells., *Farmaco.* 55 (2000) 515–20.
- [7] S.M. Halpern, A. V. Anstey, R.S. Dawe, B.L. Diffey, P.M. Farr, J. Ferguson, et al., Topical PUVA: Guidelines for Topical PUVA: A Report of A Workshop of the British Photodermatology Group, *Br. Assoc. Dermatologists' Manag. Guidel.* (2011) 284–293.
- [8] N. Kitamura, S. Kohtani, R. Nakagaki, Molecular aspects of furocoumarin reactions: Photophysics, photochemistry, photobiology, and structural analysis, *J. Photochem. Photobiol. C Photochem. Rev.* 6 (2005) 168–185.
- [9] D. Averbek, M. Dardalhon, N. Magaña-Schwencke, L.B. Meira, V. Meniel, S. Boiteux, et al., New aspects of the repair and genotoxicity of psoralen photoinduced lesions in DNA., *J. Photochem. Photobiol. B.* 14 (1992) 47–63.
- [10] S. Laube, S.A. George, Adverse effects with PUVA and UVB phototherapy., *J. Dermatolog. Treat.* 12 (2001) 101–5.
- [11] S.G.H. Otman, L.D. El-Dars, C. Edwards, E. Ansari, D. Taylor, B. Gambles, et al., Eye protection for ultraviolet B phototherapy and psoralen ultraviolet A patients., *Photodermatol. Photoimmunol. Photomed.* 26 (2010) 143–50.
- [12] J.K. Yano, M.-H. Hsu, K.J. Griffin, C.D. Stout, E.F. Johnson, Structures of human microsomal cytochrome P450 2A6 complexed with coumarin and methoxsalen., *Nat. Struct. Mol. Biol.* 12 (2005) 822–3.

- [13] M. Pradhan, D. Singh, M.R. Singh, Novel colloidal carriers for psoriasis: current issues, mechanistic insight and novel delivery approaches., *J. Control. Release.* 170 (2013) 380–95.
- [14] P. Asawanonda, N. Amornpinyokeit, C. Nimnuan, Topical 8-methoxypsoralen enhances the therapeutic results of targeted narrowband ultraviolet B phototherapy for plaque-type psoriasis., *J. Eur. Acad. Dermatol. Venereol.* 22 (2008) 50–5.
- [15] B.J. Garg, A. Saraswat, A. Bhatia, O.P. Katare, Topical treatment in vitiligo and the potential uses of new drug delivery systems., *Indian J. Dermatol. Venereol. Leprol.* 76 (2010) 231–8.
- [16] M.D. Njoo, P.I. Spuls, J.D. Bos, W. Westerhof, P.M.M. Bossuyt, Nonsurgical Repigmentation Therapies in Vitiligo, *Arch. Dermatol.* 134 (2013) 1532–1540.
- [17] I. Tegeder, L. Bräutigam, M. Podda, S. Meier, R. Kaufmann, G. Geisslinger, et al., Time course of 8-methoxypsoralen concentrations in skin and plasma after topical (bath and cream) and oral administration of 8-methoxypsoralen., *Clin. Pharmacol. Ther.* 71 (2002) 153–61.
- [18] M. Grundmann-Kollmann, M. Podda, L. Bräutigam, K. Hardt-Weinelt, R.J. Ludwig, G. Geisslinger, et al., Spatial distribution of 8-methoxypsoralen penetration into human skin after systemic or topical administration, *Br. J. Clin. Pharmacol.* 54 (2002) 535–539.
- [19] K. Borowska, S. Wołowiec, A. Rubaj, K. Głowniak, E. Sieniawska, S. Radej, Effect of polyamidoamine dendrimer G3 and G4 on skin permeation of 8-methoxypsoralene--in vivo study., *Int. J. Pharm.* 426 (2012) 280–3.
- [20] J.-Y. Fang, C.-L. Fang, C.-H. Liu, Y.-H. Su, Lipid nanoparticles as vehicles for topical psoralen delivery: Solid lipid nanoparticles (SLN) versus nanostructured lipid carriers (NLC), *Eur. J. Pharm. Biopharm.* 70 (2008) 633–640.
- [21] B. Baroli, M. a López-Quintela, M.B. Delgado-Charro, a M. Fadda, J. Blanco-Méndez, Microemulsions for topical delivery of 8-methoxsalen., *J. Control. Release.* 69 (2000) 209–18.
- [22] Y.T. Zhang, L.N. Shen, Z.H. Wu, J.H. Zhao, N.P. Feng, Comparison of ethosomes and liposomes for skin delivery of psoralen for psoriasis therapy, *Int. J. Pharm.* 471 (2014) 449–452.
- [23] Y.T. Zhang, L.N. Shen, J.H. Zhao, N.P. Feng, Evaluation of psoralen ethosomes for topical delivery in rats by using in vivo microdialysis, *Int. J. Nanomedicine.* 9 (2014) 669–678.

- [24] K. Borowska, B. Laskowska, A. Magoń, B. Mysliwiec, M. Pyda, S. Wołowicz, PAMAM dendrimers as solubilizers and hosts for 8-methoxypsoralene enabling transdermal diffusion of the guest., *Int. J. Pharm.* 398 (2010) 185–189.
- [25] M. Morgen, G.W. Lu, D. Du, R. Stehle, F. Lembke, J. Cervantes, et al., Targeted delivery of a poorly water-soluble compound to hair follicles using polymeric nanoparticle suspensions., *Int. J. Pharm.* 416 (2011) 314–22.
- [26] B. Sapra, S. Jain, K. Tiwary, Percutaneous permeation enhancement by terpenes: mechanistic view., *AAPS J.* 10 (2008) 120–132.
- [27] M. Aqil, A. Ahad, Y. Sultana, A. Ali, Status of terpenes as skin penetration enhancers, *Drug Discov. Today.* 12 (2007) 1061–1067.
- [28] T.R. Hoare, D.S. Kohane, Hydrogels in drug delivery: Progress and challenges, *Polymer.* 49 (2008) 1993–2007.
- [29] G. Feng, Y. Xiong, H. Wang, Y. Yang, Gelation of microemulsions and release behavior of sodium salicylate from gelled microemulsions., *Eur. J. Pharm. Biopharm.* 71 (2009) 297–302.
- [30] S. Alam, S. Ali, N. Alam, I. Alam, T. Anwer, F. Imam, et al., Design and Characterization of Nanostructure Topical Gel of Betamethasone Dipropionate for Psoriasis, *J. Pharm. Appl. Sci.* 2 (2012) 148–158.
- [31] M.J. Lawrence, G.D. Rees, Microemulsion-based media as novel drug delivery systems, *Adv. Drug Deliv. Rev.* 64 (2012) 175–193.
- [32] H. Chen, X. Chang, D. Du, J. Li, H. Xu, X. Yang, Microemulsion-based hydrogel formulation of ibuprofen for topical delivery., *Int. J. Pharm.* 315 (2006) 52–8.
- [33] S. Baboota, M.S. Alam, S. Sharma, J.K. Sahni, A. Kumar, J. Ali, Nanocarrier-based hydrogel of betamethasone dipropionate and salicylic acid for treatment of psoriasis., *Int. J. Pharm. Investig.* 1 (2011) 139–47.
- [34] N. Bhattarai, J. Gunn, M. Zhang, Chitosan-based hydrogels for controlled, localized drug delivery., *Adv. Drug Deliv. Rev.* 62 (2010) 83–99.
- [35] M. Dash, F. Chiellini, R.M. Ottenbrite, E. Chiellini, Chitosan—A versatile semi-synthetic polymer in biomedical applications, *Prog. Polym. Sci.* 36 (2011) 981–1014.
- [36] M.N. Ravi Kumar, A review of chitin and chitosan applications, *React. Funct. Polym.* 46 (2000) 1–27.
- [37] USP, Description and Relative Solubility, 1995.
- [38] G. Colombo, M. Artusi, P. Santi, P. Colombo, R. Bettini, A. Zucchi, et al., Skin Permeation of 5-Methoxypsoralen from Topical Dosage Forms, *Drug Dev. Ind. Pharm.*

- 29 (2003) 247–251.
- [39] C. Padula, F. Sartori, F. Marra, P. Santi, The Influence of Iontophoresis on Acyclovir Transport and Accumulation in Rabbit Ear Skin, *Pharm. Res.* 22 (2005) 1519–1524.
- [40] K. Moser, K. Kriwet, A. Naik, Y.N. Kalia, R.H. Guy, Passive skin penetration enhancement and its quantification in vitro, *Eur. J. Pharm. Biopharm.* 52 (2001) 103–112.
- [41] A. Said, S. Makki, P. Muret, J.-C. Rouland, G. Toubin, J. Millet, Lipophilicity Determination of Psoralens Used in Therapy through Solubility and Partitioning: Comparison of Theoretical and Experimental Approaches, *J. Pharm. Sci.* 85 (1996) 387–392.
- [42] A. Azeem, M. Rizwan, F.J. Ahmad, Z. Iqbal, R.K. Khar, M. Aqil, et al., Nanoemulsion components screening and selection: a technical note., *AAPS PharmSciTech.* 10 (2009) 69–76.
- [43] C.R.E. Senna, J.P., Ricci-Junior, E., Mansur, Development and Evaluation of Nanoemulsions Containing Phthalocyanines for Use in Photodynamic Cancer Therapy, *J. Nanosci. Nanotechnol.* 15 (2015) 4205–4214.
- [44] A. Gupta, H.B. Eral, T.A. Hatton, P.S. Doyle, Controlling and predicting droplet size of nanoemulsions: scaling relations with experimental validation, *Soft Matter.* 12 (2016) 1452–1458.
- [45] T. Tadros, P. Izquierdo, J. Esquena, C. Solans, Formation and stability of nanoemulsions, *Adv. Colloid Interface Sci.* 108-109 (2004) 303–318.
- [46] A. Torcello-Gómez, M. Wulff-Pérez, M.J. Gálvez-Ruiz, A. Martín-Rodríguez, M. Cabrerizo-Vílchez, J. Maldonado-Valderrama, Block copolymers at interfaces: Interactions with physiological media, *Adv. Colloid Interface Sci.* 206 (2014) 414–427.
- [47] M.H. Shahavi, M. Hosseini, M. Jahanshahi, R.L. Meyer, G.N. Darzi, Evaluation of critical parameters for preparation of stable clove oil nanoemulsion, *Arab. J. Chem.* (2015).
- [48] S. Gupta, S.P. Moulik, S. Lala, M.K. Basu, S.K. Sanyal, S. Datta, Designing and testing of an effective oil-in-water microemulsion drug delivery system for in vivo application., *Drug Deliv.* 12 (2005) 267–73.
- [49] L. Salvia-Trujillo, A. Rojas-Graü, R. Soliva-Fortuny, O. Martín-Belloso, Physicochemical characterization and antimicrobial activity of food-grade emulsions and nanoemulsions incorporating essential oils, *Food Hydrocoll.* 43 (2015) 547–556.
- [50] M.K. Anwer, S. Jamil, E.O. Ibnouf, F. Shakeel, Enhanced antibacterial effects of clove

- essential oil by nanoemulsion., *J. Oleo Sci.* 63 (2014) 347–54.
- [51] D.M. Mostafa, S.H.A. El-Alim, M.H. Asfour, S.Y. Al-Okbi, D.A. Mohamed, G. Awad, Transdermal nanoemulsions of *Foeniculum vulgare* Mill. essential oil: Preparation, characterization and evaluation of antidiabetic potential, *J. Drug Deliv. Sci. Technol.* 29 (2015) 99–106.
- [52] T.N. Barradas, V.E.B. de Campos, J.P. Senna, C. dos S.C. Coutinho, B.S. Tebaldi, K.G. de H. e Silva, et al., Development and characterization of promising o/w nanoemulsions containing sweet fennel essential oil and non-ionic surfactants, *Colloids Surfaces A Physicochem. Eng. Asp.* 480 (2015) 214–221.
- [53] D. Carreau, D. Bassani, I. Pianet, The “Ouzo effect”: Following the spontaneous emulsification of trans-anethole in water by NMR, *Comptes Rendus Chim.* 11 (2008) 493–498.
- [54] P. Alexandridis, J.F. Holzwarth, T.A. Hatton, Micellization of Poly (ethylene oxide ) -Poly (propylene oxide ) -Poly (ethylene oxide ) Triblock Copolymers in Aqueous Solutions : Thermodynamics of Copolymer Association, *Macromolecules.* 27 (1994) 2414–2425.
- [55] D. a Chiappetta, A. Sosnik, Poly(ethylene oxide)-poly(propylene oxide) block copolymer micelles as drug delivery agents: improved hydrosolubility, stability and bioavailability of drugs., *Eur. J. Pharm. Biopharm.* 66 (2007) 303–17.
- [56] ICH, Validation of analytical procedures: text and methodology Q2(R1), 2005.
- [57] ICH, Guidance for Industry Q1A(R2) Stability Testing of New Drug Substances and Products, 2003.
- [58] C.A. Kienzle-Sterzer, D. Rodriguez-Sanchez, C.K. Rha, Flow behavior of a cationic biopolymer: Chitosan, *Polym. Bull.* 13 (1985).
- [59] C. Anchisi, A.M. Maccioni, M. Cristina Meloni, Physical properties of chitosan dispersions in glycolic acid., *Farmaco.* 59 (2004) 557–61.
- [60] N. Calero, J. Muñoz, P. Ramírez, A. Guerrero, Flow behaviour, linear viscoelasticity and surface properties of chitosan aqueous solutions, *Food Hydrocoll.* 24 (2010) 659–666.
- [61] A. V. Mironov, G.A. Vikhoreva, N.R. Kil’deeva, S.A. Uspenskii, Reasons for unstable viscous properties of chitosan solutions in acetic acid, *Polym. Sci. Ser. B.* 49 (2007) 15–17.
- [62] A. Ahad, M. Aqil, A. Ali, The application of anethole, menthone, and eugenol in transdermal penetration of valsartan: Enhancement and mechanistic investigation,

Pharm. Biol. (2015) 1–10.

- [63] M.A. Bolzinger, C. Carduner, Thevenin, M., Poelman, Bicontinuous sucrose ester microemulsion: a new vehicle for topical delivery of niflumic acid, *Int. J. Pharm.* 176 (1998) 39–45.

## Figure Captions

**Figure 1:** Average droplet diameter of nanoemulsions (NE) containing clove oil and 8-MOP

**Figure 2:** Average droplet diameter of nanoemulsions (NE) containing sweet fennel oil and 8-MOP

**Figure 3:** pH for NE and HTN based on clove and sweet fennel essential oils after heating-freezing cycles and 11.000 rpm centrifugation.

**Figure 4:** Average droplet diameter of NE containing sweet fennel oil (NEF) and clove oil (NEC) after heating-freezing cycles and 11.000 rpm centrifugation.

**Figure 5:** pH for NE and HTN based on clove and sweet fennel essential after 15, 30, 60 and 90 days under 45°C.

**Figure 6:** Flow curves under continuous shear rate ramps of 0.01 to 100 s<sup>-1</sup> for formulations based on clove essential oil after 15, 30, 60 and 90 days under 45°C.

**Figure 7:** Flow curves under continuous shear rate ramps of 0.01 to 100 s<sup>-1</sup> for formulations based on sweet fennel essential oil after 15, 30, 60 and 90 days under 45°C.

**Figure 8:** Average droplet diameter for formulations based on clove and sweet fennel essential oil after 15, 30, 60 and 90 days under 45°C

**Figure 9:** 8-MOP permeation profiles across pig ear skin from NEC, NEF and control sample (n=6). Mean values ± S.E.M.

**Figure 10:** 8-MOP permeation profiles across pig ear skin (A) and skin acumulation from formulations based on clove oil under infinite dosing conditions (n=6). Mean values ± S.E.M.

**Figure 11:** 8-MOP permeation profiles across pig ear skin (A) and skin acumulation from formulations based on sweet fennel oil under infinite dosing conditions (n=6). Mean values ± S.E.M.

**Figure 12:** Transmission Electron Microscopy for NEC (A), NEF (B) and NHF1 (C). Magnification 2000x.

**Figure 13:** 8-MOP skin acumulation from formulations based on clove (A) and sweet fennel essential oil (B) under finite dosing conditions (n=6). Mean values ± S.E.M.

## **Table Titles**

**Table 1:** Results from Solubility Tests

**Table 2:** Composition and pH of produced formulations

**Table 3:** Results from accelerated stability studies of formulations regarding Color /Odor alterations

**Table 4:** Permeation parameters and pH determined for formulations containing clove oil, and sweet fennel oil.

**Table 1**

| <b>Essential oil</b> | <b>8-MOP Solubility</b> |
|----------------------|-------------------------|
| <b>Sweet Fennel</b>  | Freely Soluble (>20%)   |
| <b>Mint</b>          | Soluble (10%)           |
| <b>Bitter orange</b> | Insoluble               |
| <b>Sweet orange</b>  | Insoluble               |
| <b>Lime</b>          | Soluble (10%)           |
| <b>Buriti</b>        | Insoluble               |
| <b>Avocado</b>       | Insoluble               |
| <b>Clove</b>         | Freely Soluble (>20%)   |
| <b>Copaiba</b>       | Insoluble               |

**Table 2**

| <b>Oil Phase (5%)</b> | <b>Surfactant (wt%)</b> | <b>Chitosan (2%)</b> | <b>Sample</b> | <b>pH ± SD</b>     |
|-----------------------|-------------------------|----------------------|---------------|--------------------|
| Clove oil             | Pluronic F68 (10%)      | -                    | <b>NEC</b>    | <b>5.39 ± 0.03</b> |
|                       |                         | Low MW(2%)           | <b>NHC1</b>   | <b>5.16 ± 0.08</b> |
|                       |                         | Medium MW            | <b>NHC2</b>   | <b>4.62 ± 0.07</b> |
|                       |                         | High MW              | <b>NHC3</b>   | <b>4.48 ± 0.04</b> |
| Sweet Fennel oil      | Cremophor RH 40 (3%)    | -                    | <b>NEF</b>    | <b>5.43 ± 0.02</b> |
|                       |                         | Low MW               | <b>NHF1</b>   | <b>4.72 ± 0.1</b>  |
|                       |                         | Medium MW            | <b>NHF2</b>   | <b>4.45 ± 0.09</b> |
|                       |                         | High MW              | <b>NHF3</b>   | <b>4.26 ± 0.13</b> |

**Table 3**

| <b>Sample</b> | <b>Color/odor<br/>Initial</b> | <b>Color/odor<br/>After 15 days</b> | <b>Color/odor<br/>After 30 days</b> | <b>Color/odor<br/>After 60 days</b> | <b>Color/odor<br/>After 90 days</b> |
|---------------|-------------------------------|-------------------------------------|-------------------------------------|-------------------------------------|-------------------------------------|
| <b>NEC</b>    | <b>I</b>                      | <b>I</b>                            | <b>I</b>                            | <b>I</b>                            | <b>I</b>                            |
| <b>NHC1</b>   | <b>I</b>                      | <b>I</b>                            | <b>I</b>                            | <b>II</b>                           | <b>II</b>                           |
| <b>NHC2</b>   | <b>I</b>                      | <b>I</b>                            | <b>I</b>                            | <b>II</b>                           | <b>II</b>                           |
| <b>NHC3</b>   | <b>I</b>                      | <b>I</b>                            | <b>I</b>                            | <b>II</b>                           | <b>II</b>                           |
| <b>NEF</b>    | <b>I</b>                      | <b>I</b>                            | <b>I</b>                            | <b>I</b>                            | <b>I</b>                            |
| <b>NHF1</b>   | <b>I</b>                      | <b>I</b>                            | <b>I</b>                            | <b>I</b>                            | <b>I</b>                            |
| <b>NHF2</b>   | <b>I</b>                      | <b>I</b>                            | <b>I</b>                            | <b>I</b>                            | <b>I</b>                            |
| <b>NHF3</b>   | <b>I</b>                      | <b>I</b>                            | <b>I</b>                            | <b>I</b>                            | <b>I</b>                            |

**Table 4**

| <b>Formulation</b> | <b>KH (cm)</b> | <b>D/H<sup>2</sup> (h<sup>-1</sup>)</b> | <b>P (cm h<sup>-1</sup>) *10<sup>3</sup></b> | <b>Time lag (h)</b> |
|--------------------|----------------|---|--|---------------------|
| <b>Control</b>     | 0.043 (0.021)  | 0.110 (0.104)                           | 3.15 (0.36)                                  | 2.2 (1.0)           |
| <b>NEC</b>         | 0.071 (0.023)  | 0.043 (0.004)                           | 2.97 (0.89)                                  | 3.9 (0.3)           |
| <b>NHC1</b>        | 0.011 (0.008)  | 0.082 (0.031)                           | 0.73 (0.18)                                  | 2.4 (1.4)           |
| <b>NHC2</b>        | 0.017 (0.008)  | 0.061 (0.030)                           | 0.92 (0.28)                                  | 3.3 (1.4)           |
| <b>NHC3</b>        | 0.009 (0.002)  | 0.065 (0.012)                           | 0.55 (0.08)                                  | 2.7 (0.6)           |
| <b>NEF</b>         | 0.090 (0.027)  | 0.088 (0.045)                           | 7.29 (2.61)                                  | 2.3 (1.1)           |
| <b>NHF1</b>        | 0.215 (0.079)  | 0.124 (0.082)                           | 22.38 (5.00)                                 | 1.7 (0.6)           |
| <b>NHF2</b>        | 0.269 (0.113)  | 0.094 (0.061)                           | 21.78 (13.25)                                | 4.0 (5.2)           |
| <b>NHF3</b>        | 0.223 (0.093)  | 0.232 (0.180)                           | 39.86 (6.06)                                 | 1.0 (0.4)           |

Figure 1

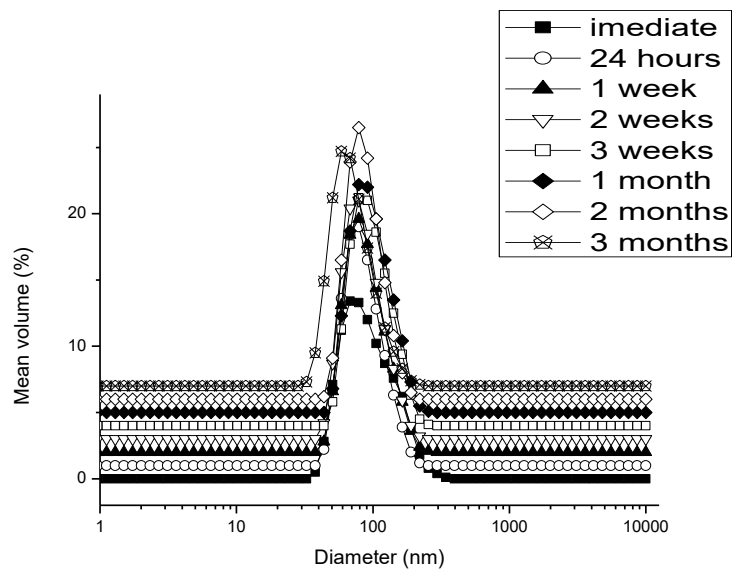


Figure 2

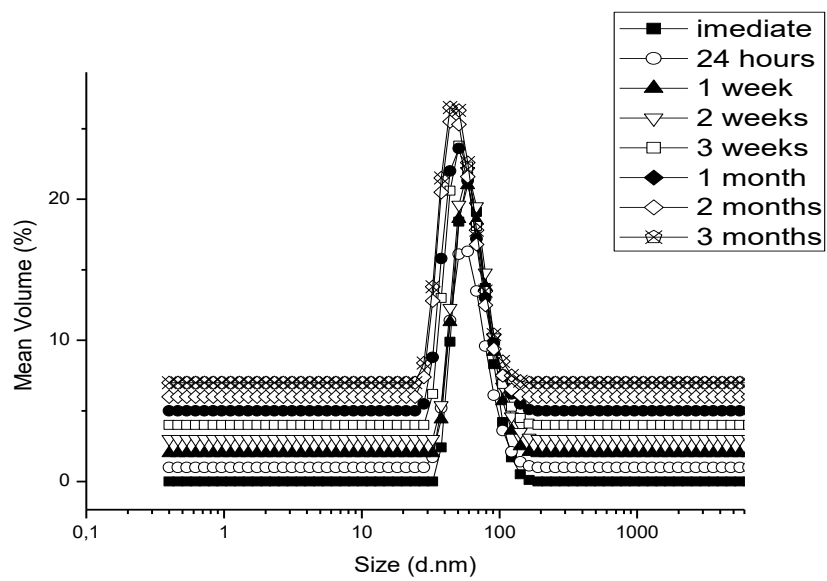


Figure 3

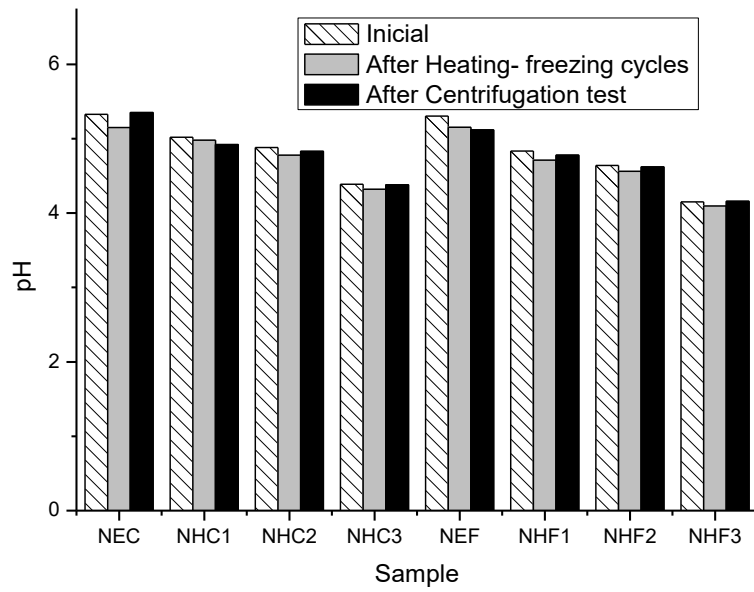


Figure 4

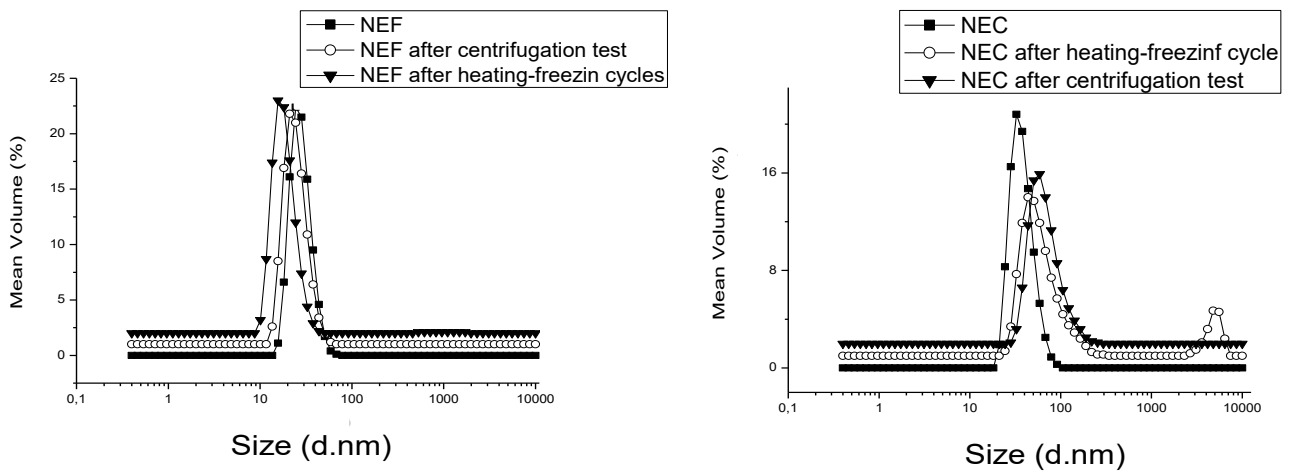


Figure 5

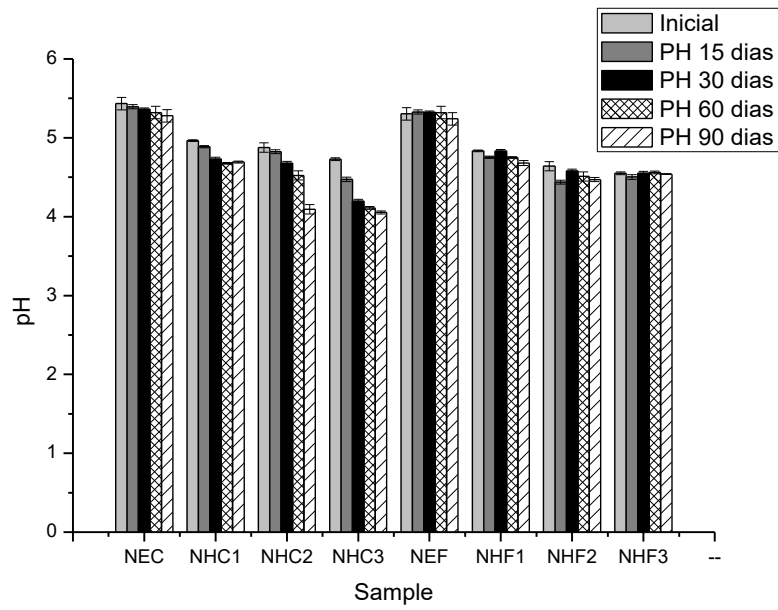


Figure 6

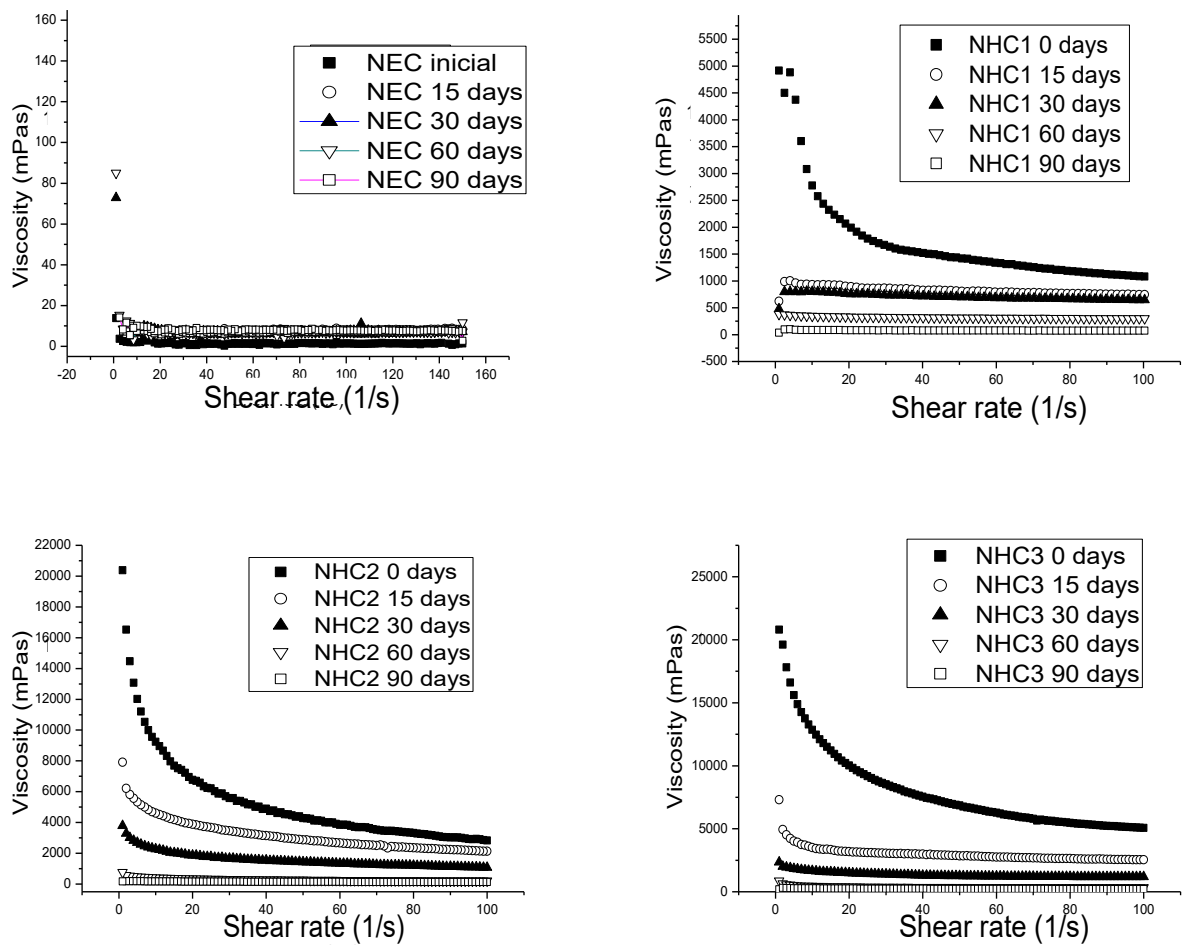


Figure 7

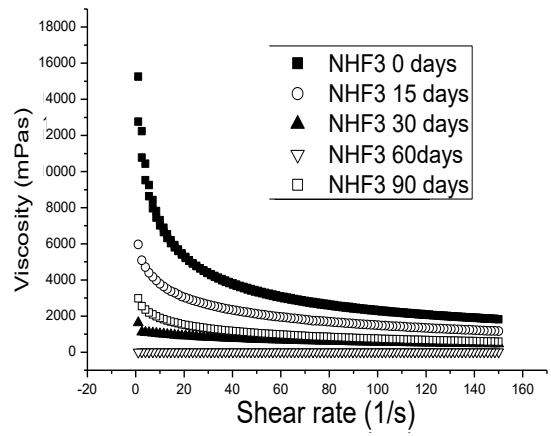
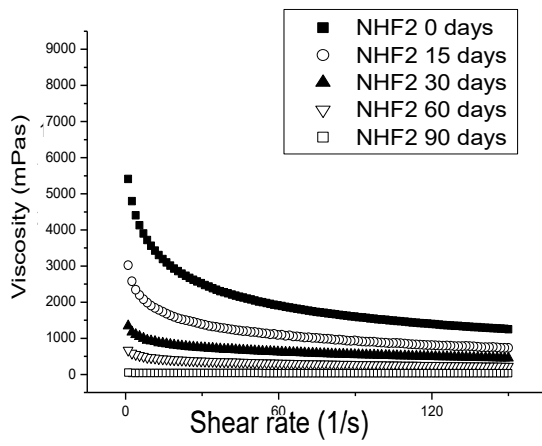
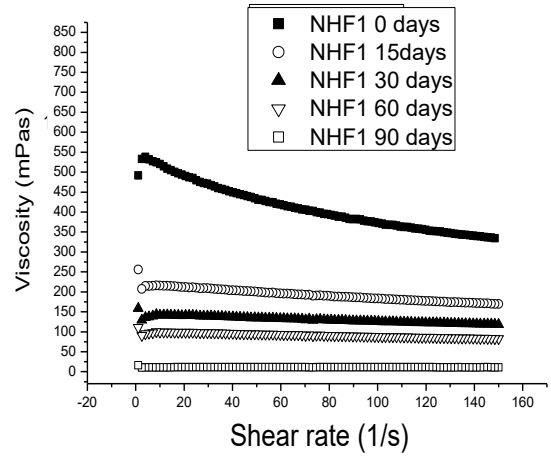
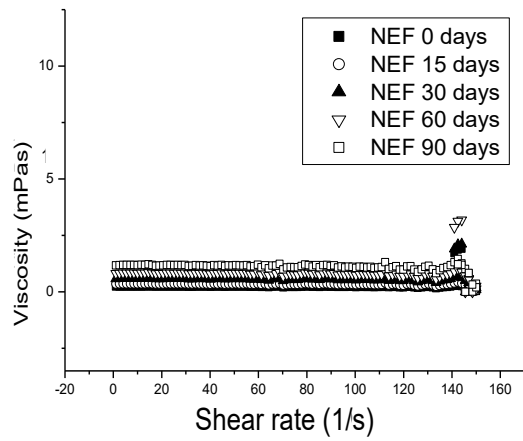


Figure 8

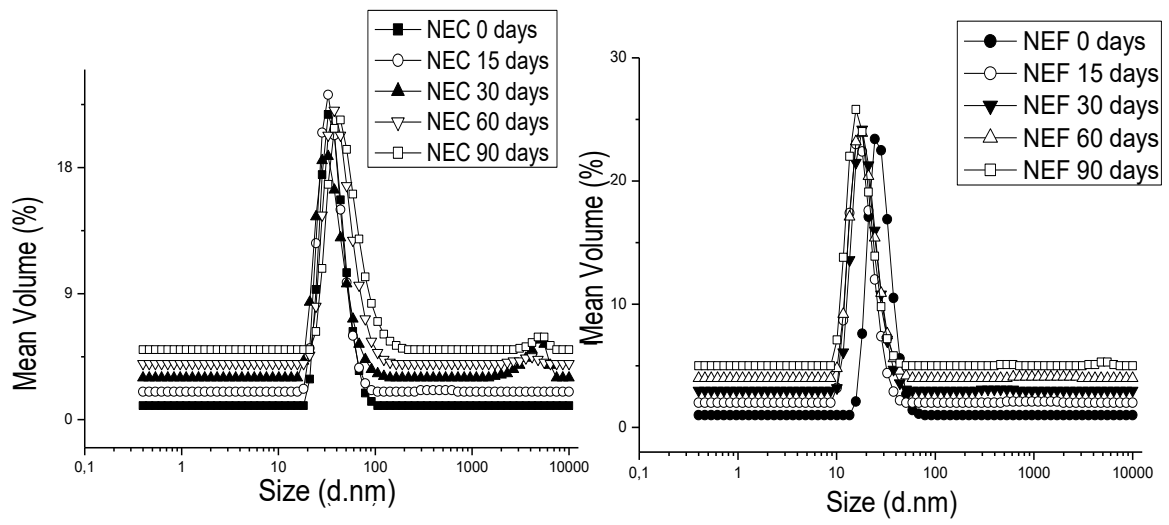


Figure 9

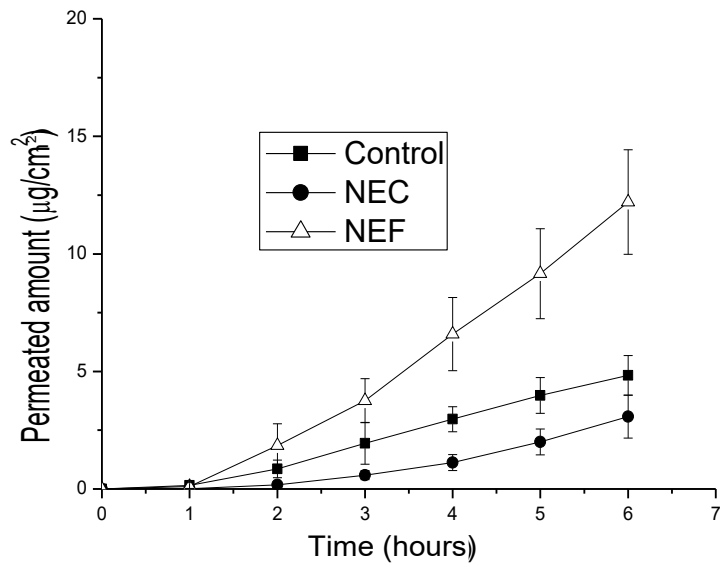


Figure 10

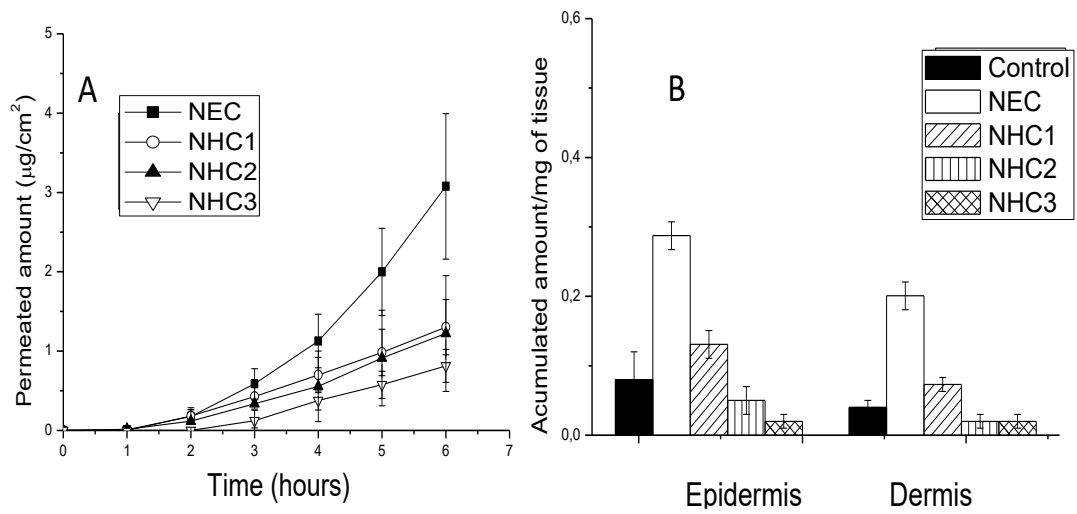


Figure 11

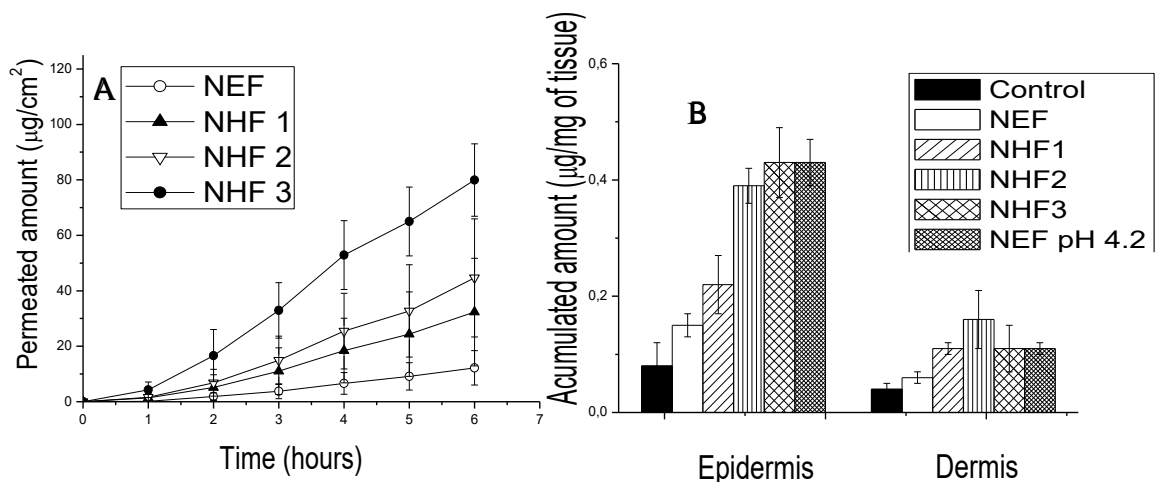


Figure 12

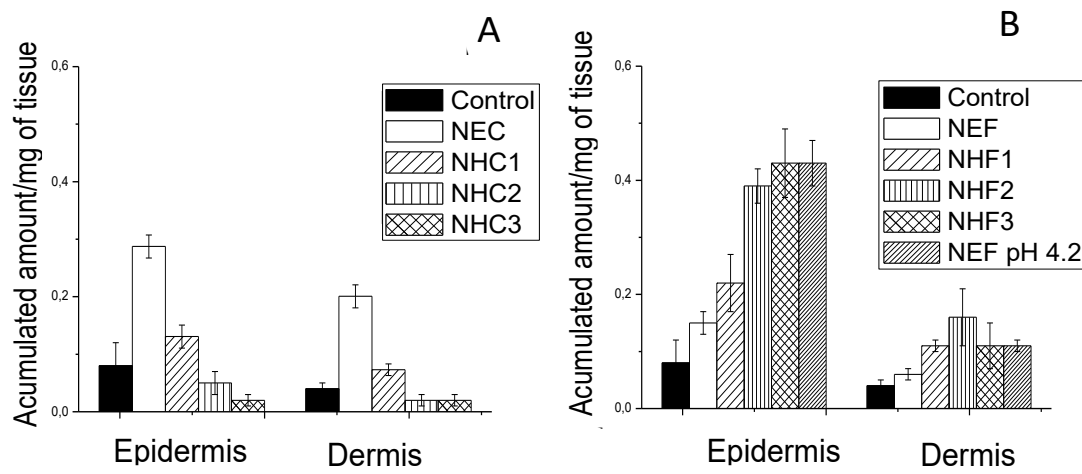


Figure 13

